Journal of Solid State Chemistry **166,** 229–236 (2002)
doi:10.1006/jssc.2002.9588, available online at http://www.idealibrary.com on IDEAL®

XANES Study on the Generation and Distribution of Holes via Ca Substitution and O Doping in $Cu(Ba_{0.8}Sr_{0.2})_2(Yb_{1-x}Ca_x)Cu_2O_{6+z}$

M. Karppinen,*,[1] H. Yamauchi,* T. Nakane,* K. Fujinami,* K. Lehmus,† P. Nachimuthu,‡ R. S. Liu,‡ and J. M. Chen§

*Materials and Structures Laboratory, Tokyo Institute of Technology, Yokohama 226-8503, Japan; †Laboratory of Inorganic and Analytical Chemistry, Helsinki University of Technology, FIN-02015 Espoo, Finland; ‡Department of Chemistry, National Taiwan University, Taipei, Taiwan, Republic of China; §Synchrotron Radiation Research Center, Hsinchu, Taiwan, Republic of China

Received November 28, 2001; received in revised form March 1, 2002; accepted March 15, 2002

Generation of holes is facilitated in the $Cu(Ba_{0.8}Sr_{0.2})_2(Yb_{1-x}Ca_x)Cu_2O_{6+z}$ (Cu-1212) system by two independent ways, i.e., by Ca substitution ($0 \le x \le 0.35$) and O doping ($0 < z < 1$). The distribution of holes between the CuO_2–$(Yb_{1-x}Ca_x)$–CuO_2 block containing two identical superconductive CuO_2 planes and the "charge-reservoir" block consisting of a single CuO_z chain has been quantitatively investigated by means of O *K*-edge and Cu $L_{2,3}$-edge X-ray absorption near-edge structure (XANES) spectroscopy. The resultant values for the CuO_2-plane hole concentration are compared with those calculated employing the bond-valence-sum (BVS) method from the neutron powder diffraction (NPD) data previously reported for the same samples. The results of the two methods are in good agreement. The two independent hole-doping ways are found to result in different distributions of holes over the crystal, i.e., different ratios of hole numbers at the CuO_2 plane and the CuO_z chain. With Ca substitution holes are directed efficiently into the CuO_2 plane, while for O doping holes are more homogeneously distributed between the CuO_2 plane and the CuO_z chain. Moreover, the value of T_c at a fixed CuO_2-plane hole concentration is shown to be higher for Ca-substituted than for O-doped samples.

Key Words: **XANES spectroscopy; hole distribution; Cu-1212 superconductor.**

INTRODUCTION

Most of the known high-T_c superconductive copper oxide phases obey a general formula of $M_mA_2Q_{n-1}Cu_nO_{m+2+2n-\delta}$. The basic structure of a multi-layered $M_mA_2Q_{n-1}Cu_nO_{m+2+2n-\delta}$ phase contains alternating $M_mO_{m-\delta}$ "charge-reservoir" blocks with m $MO_{1-\delta/m}$ oxide layers (M = Cu, Bi, Pb, Tl, Hg, Al, Ga, C, and B) and superconductive $Q_{n-1}Cu_nO_{2n}$ blocks with n CuO_2 planes and $n-1$ Q metal layers (Q = Ca, R; R = rare-earth element). The $M_mO_{m-\delta}$ charge-reservoir block is separated from the $Q_{n-1}Cu_nO_{2n}$ block by a single AO layer (A = Sr, Ba, and La), such that the crystal structure is constructed by the repetition of the layer sequence, –CuO_2–$(Q$–$CuO_2)_{n-1}$–AO–$(MO_{1-\delta/m})_m$–AO– (1). Note that only the $M_mO_{m-\delta}$ charge-reservoir block is non-stoichiometric in terms of oxygen. Each $M_mA_2Q_{n-1}Cu_nO_{m+2+2n-\delta}$ phase is denoted in an unambiguous way by M-$m^{(A)}2^{(Q)}(n$-1)n, though the shorter names, M-$m2(n$-1)n, are more commonly used (1). According to this general notation, the systematic name for the $Cu(1)Ba_2RCu(2)_2O_{7-\delta}$ or the so-called "R-123" phase is Cu-$1^{(Ba)}2^{(R)}$12 or Cu-1212.

For an $M_mA_2Q_{n-1}Cu_nO_{m+2+2n-\delta}$ phase, the "nominal average hole concentration" in the superconductive CuO_2 plane(s) of the $Q_{n-1}Cu_nO_{2n}$ block is determined at a certain stoichiometry of the cations, M, A and Q, by the amount of oxygen in the $M_mO_{m-\delta}$ charge reservoir (1). However, in most cases, establishment of oxygen stoichiometry, i.e., δ in $M_mO_{m-\delta}$, does not define the "actual hole concentration" in the CuO_2 plane(s) in an unambiguous way. In the $Cu(1)Ba_2RCu(2)_2O_{6+z}$ (here we use "$6+z$" instead of "7-δ") structure, the distribution of holes over the charge-reservoir $Cu(1)O_z$ chain and the $Cu(2)O_2$ plane in the superconductive block is non-trivial, and cannot be evaluated solely from the result of oxygen-content analysis. Also, in the case of e.g., Bi-, Pb- and Tl-containing charge-reservoir blocks the actual hole concentration in the CuO_2 plane(s) depends not only on the amount of excess oxygen but also on the exact (non-integer) oxidation state of the cation constituent(s) M in $M_mO_{m-\delta}$ (1, 2). Determining the distinct hole concentrations of each structural block explicitly is essential to be able to understand the dependence of the properties such as the superconductivity transition temperature (T_c) and the irreversibility field of

[1]To whom correspondence should be addressed. Fax: +81-45-924-5365. E-mail: karppinen@rlem.titech.ac.jp.

0022-4596/02 $35.00

magnetization (H_{irr}) on the hole distribution over the different layers/blocks of the multi-layered copper oxide crystal (1). Also, it is important to establish the chemical ways to control the hole-concentration distribution (3).

In the present contribution, the distribution of holes in the $Cu(Ba_{0.8}Sr_{0.2})_2(Yb_{1-x}Ca_x)Cu_2O_{6+z}$ system of the Cu-1212 phase is determined by means of O *K*-edge and Cu $L_{2,3}$-edge X-ray absorption near-edge structure (XANES) spectroscopy. The XANES technique utilizing synchrotron radiation has been recognized as a powerful tool for investigating the concentration of unoccupied states at the copper and oxygen sites in superconductive copper-oxide crystals. Most importantly, based on polarization-dependent XANES studies on $CuBa_2YCu_2O_{6+z}$ single crystals with various different oxygen contents, Nücker *et al.* (4) established in 1995 the assignment of the multiple pre-edge peaks in the O *K*-edge spectra originating from the different binding energies of O 1*s* levels of unequivalent oxygen sites. Recently, changes in site-specific hole concentrations were also followed with varying cation-substitution level in $Cu(Ba,Nd)_2NdCu_2O_{6+z}$, $CuBa_2(Y,Pr)Cu_2O_{6+z}$, $Cu(Ba,Sr)_2YCu_2O_{6+z}$, $Bi_2Sr_2(Ca,Y)Cu_2O_{8+\delta}$ and $(Pb_{2/3}Cu_{1/3})_3Sr_2(Y,Ca)Cu_2O_{8+z}$ powder samples and in $CuBa_2(Y,Ca)Cu_2O_{6+z}$ single crystals by O *K*-edge XANES measurements (5–13). In the present O *K*-edge and Cu $L_{2,3}$-edge XANES study on the $Cu(Ba_{0.8}Sr_{0.2})_2(Yb_{1-x}Ca_x)Cu_2O_{6+z}$ system, effects of two independent hole-doping ways, i.e., Ca^{II}-for-Yb^{III} substitution (increasing x) and O doping (increasing z), facilitated in the same parent structure with wide doping ranges, are systematically compared. Note that for the $CuA_2(R_{1-x}Ca_x)Cu_2O_{6+z}$ system with $A=(Ba_{0.8}Sr_{0.2})$ and $R=Yb$, the solubility limit of Ca extends up to $x=0.35-0.40$ (14, 15) enabling us to study doping effects for a wide Ca-substitution range. The oxygen content was varied in the range of $0\le z\le 0.96$ in the samples studied. Furthermore, the results for the layer-specific hole concentrations obtained for the $Cu(Ba_{0.8}Sr_{0.2})_2(Yb_{1-x}Ca_x)Cu_2O_{6+z}$ system from the O *K*-edge XANES data are compared with the results of bond-valence-sum (BVS) calculations based on precise structural data obtained for the same sample powders from neutron powder diffraction (NPD) experiments (16). The present notation system for the atoms in the $Cu(Ba,Sr)_2(Yb,Ca)Cu_2O_{6+z}$ structure follows that of Ref. (16) and is given in Fig. 1.

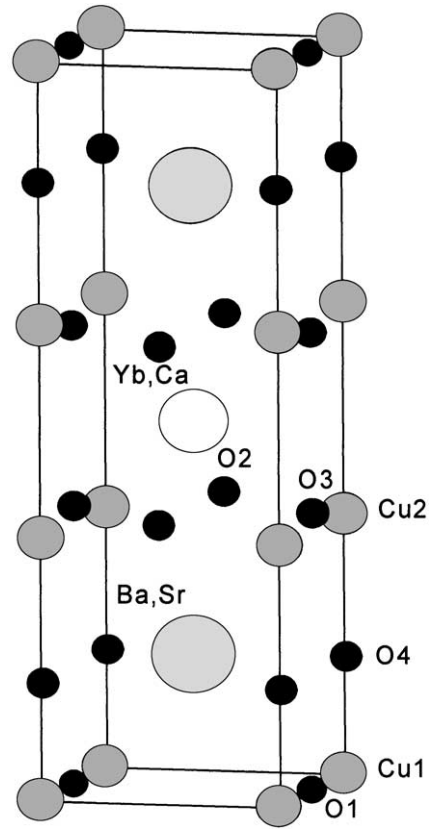

FIG. 1. Schematic presentation of the $Cu(Ba,Sr)_2(Yb,Ca)Cu_2O_{6+z}$ structure and the present notation system for the atoms.

EXPERIMENTAL

Synthesis and Characterization of the Samples

For XANES measurements, $Cu(Ba_{0.8}Sr_{0.2})_2(Yb_{1-x}Ca_x)Cu_2O_{6+z}$ single-phase samples with $x=0$, 0.10, 0.25 and 0.35, and z in a range of 0–0.96 were used. The samples were prepared from Yb_2O_3, $BaCO_3$, $SrCO_3$, $CaCO_3$ and CuO utilizing the technique including an unconventional post-annealing procedure (the so-called TCOD (1) method) as described elsewhere in detail (15, 16). In brief, cation-stoichiometric mixtures of the starting materials were calcined several times, sintered in a pelletized form in air at 900–940°C, and then annealed in powder form in O_2 at 350°C for 48 h. Oxygen-deficient samples were obtained from the as-prepared materials by post-annealing in an Ar atmosphere at different temperatures between 380°C and 800°C. In order to ensure the homogeneity of the oxygen content in the whole sample, these post-annealings were carried out in powder form for a small batch of 150–200 mg using a slow heating rate (2°C/min) and employing an isothermal heating period of 6 h at the final temperature. All the post-annealings were performed in a thermobalance of high sensitivity (MAC Science: TG/DTA 2000 S). Consequently, it was possible to carefully control temperature and atmosphere during the oxygen-depletion procedure and to detect in situ the change in the weight/oxygen stoichiometry. Finally, the exact oxygen contents were established by the coulometric Cu^+/Cu^{2+} titration method (2, 15, 16). The phase purity of the synthesized samples was confirmed by X-ray diffraction (XRD; MAC Science:

MXP18VAHF[22]; Cu$K\alpha$ radiation). The same samples were characterized for the precise crystallographic structures by neutron powder diffraction experiments carried out at R2 reactor in Studsvik, Sweden. The experimental procedures and the results obtained thereby are discussed in detail elsewhere (16). [Note that for the NPD experiments, 10–20 parallel TG annealings were performed to collect a large enough sample amount.] The T_c values reported for the samples were taken at the onset temperatures of diamagnetic signal in SQUID measurements (Quantum Design: MPMS-5S) carried out down to 5 K in a field-cooling mode with a magnetic field of 10 Oe.

The O *K*-edge and Cu $L_{2,3}$-edge XANES measurements were performed on 6-m high-energy spherical grating monochromator (HSGM) beam-line at Synchrotron Radiation Research Center (SRRC) in Hsinchu, Taiwan. The X-ray fluorescence-yield spectra were recorded from powder samples at room temperature using a microchannel-plate (MCP) detector system consisting of a dual set of MCPs with an electrically isolated grid mounted in front of them. The grid was set to a voltage of 100 V, the front of the MCPs to −2000 V and the rear to −200 V. The grid bias ensured that positive ions did not enter the detector, while the MCP bias ensured that no electrons were detected. The detector was located parallel to the sample surface at a distance of ~2 cm. Photons were incident at an angle of 45° with respect to the sample normal. The incident photon flux (I_0) was monitored simultaneously by a Ni mesh located after the exit slit of the monochromator. All the absorption measurements were normalized to I_0. The photon energies were calibrated with an accuracy of 0.1 eV using the O *K*-edge absorption peak at 530.1 eV and the Cu L_3 white line at 931.2 eV of a CuO reference. The monochromator resolution was set to ~0.22 and ~0.45 eV at the O *K* (1*s*) and Cu $L_{2,3}$ (2*p*) absorption edges, respectively. The X-ray fluorescence-yield method applied here is bulk-sensitive, the probing depth being estimated at 1000–5000 Å.

Assignment of the Pre-edge Peaks in the O K-Edge and Cu $L_{2,3}$-Edge Spectra

The pre-edge features in the O *K*-edge spectra were assigned and analyzed in the way parallel to that applied in Refs. (4–10). The peaks originating from the hole states at the apical oxygen site (O(4)) and at the oxygen atom in the CuO_z chain (O(1)) are found superimposed at ~527.5 eV, while the peak at ~528.2 eV is attributed to the oxygen hole states in the CuO_2 plane. For reference, the energy value of ~528.2 eV for the oxygen hole states in the present pyramidal CuO_2 planes with copper at a mixed $Cu^{II/III}$ oxidation state may be compared to that of 528.8 eV reported for the isolated square-planar planes of Cu^{III} in $La_2Li_{0.5}Cu_{0.5}O_4$ (17). The peak at ~529.2 eV is due to the oxygen states hybridized with the upper Hubbard band (UHB). The peaks were analyzed by fitting Gaussian functions to each spectrum. Before fitting, each spectrum was normalized to have the same intensity for the main peak at ~537.5 eV. Furthermore, after fitting the integrated intensities of the pre-edge peaks were multiplied by the exact oxygen content $6+z$ of the sample as established by wet-chemical analysis. The thus obtained intensities for the peaks at ~527.5 eV ($I_{527.5}$) and at ~528.2 eV ($I_{528.2}$) were supposed to reflect the hole concentrations in the CuO_z chain and the two CuO_2 planes of the unit cell, respectively (4).

In the Cu $L_{2,3}$-edge absorption spectra, the two strong and narrow peaks around 931 and 951 eV are due to Cu^{II}, i.e., transitions $3d^9 \rightarrow \underline{2p}^1 3d^{10}$. Both the peaks show shoulders on the high-energy side in highly oxidized samples. These shoulders, first reported by Bianconi *et al.* (18) for $CuBa_2YCu_2O_{6+z}$, have been interpreted as transitions $3d^8 \rightarrow \underline{2p}^1 3d^{10}\underline{L}$ ($\underline{L}$ denotes a ligand hole in the O 2*p* orbital) and are supposed to reflect the total concentration of holes, i.e., being due to Cu^{III}. Especially, the shoulder of the ~931 eV peak at ~932.6 eV (for reference, at 932.7 eV in $La_2Li_{0.5}Cu_{0.5}O_4$, i,e., shifted by 1.7eV from the peak due to Cu^{II} (17)) is clearly distinguishable in the O-doped $Cu(Ba_{0.8}Sr_{0.2})_2YbCu_2O_{6+z}$ samples allowing the quantitative analysis of the amount of Cu^{III}. The analysis of the L_3 area of the Cu $L_{2,3}$-edge spectra was done by fitting the peaks with Gaussian functions and normalizing the integrated intensity of the shoulder against the total spectral weight. The peak near 934 eV was assigned to Cu^{I} at the Cu(1) site since a similar peak is characteristically observed in compounds of Cu^{I} with two-fold oxygen coordination (4, 19). In $Cu(1)Ba_2YCu(2)O_{6+z}$, it was explained by Nücker *et al.* (4) to originate from the hybridization of Cu(1) 4*p* or 4*s* states with Cu(1) $3d_{z2-r2}$ orbitals and apical O(4) $2p_z$ orbitals.

Calculation of the Hole Concentrations

To discuss the O *K*-edge XANES data obtained for the layer-specific hole concentrations, the results are compared with the hole concentration values calculated for the CuO_2 plane by the bond-valence-sum method. The BVSs for the in-plane copper and oxygen atoms were calculated according to the scheme by Brown and Altermatt (20), i.e., first the bond-valence s_{ij} of each *i*–*j* bond from an empirically determined parameter R_{ij}^0 and the experimental bond length d_{ij} (in Å), by

$$s_{ij} = e^{(R_{ij}^0 - d_{ij})/0.37} \qquad [1]$$

and then the BVS around a species *i* by summing over the bond valences from all the nearest-neighboring

counter-ions as

$$V_i = \pm \sum_j s_{ij}. \quad [2]$$

The following R_{ij}^0 values were used: 1.965 for Yb–O, 1.967 for Ca–O, 2.285 for Ba–O and 2.118 for Sr–O (20). For the Cu–O bonds with copper in intermediate oxidation states the $R_{\mathrm{Cu-O}}^0$ values were iterated in a self-consistent way supposing that the value of $R_{\mathrm{Cu-O}}^0$ depends linearly on the oxidation number of Cu in between the limit values of 1.679 for Cu^{II} and 1.730 for Cu^{III}. For the d_{ij} values, those calculated from the NPD data of Ref. (16) were utilized. The calculated V_i sum was given as a positive value for the copper atom and as a negative value for the oxygen atom(s).

In the superconductive $M_mA_2Q_{n-1}Cu_nO_{m+2+2n-\delta}$ phases, the excess positive charge in a superconductive CuO_2 plane(s) is likely to be delocalized. Therefore, the BVS estimation for the CuO_2-plane hole concentration ($p_{\mathrm{BVS,plane}}$) was calculated from the V_i's obtained for the in-plane copper and oxygen atoms by summing the holes on one copper atom ($p_{\mathrm{Cu}} = V_{\mathrm{Cu}} - 2$) and two oxygen atoms ($p_{\mathrm{O}} = V_{\mathrm{O}} + 2$) in one CuO_2 unit in a way first suggested by Tallon (21):

$$p_{\mathrm{BVS,plane}} = V_{\mathrm{Cu}} + V_{\mathrm{O(2)}} + V_{\mathrm{O(3)}} + 2. \quad [3]$$

Note that in orthorhombic structures O(2) and O(3) indicate oxygen atoms along the *a*- and *b*-axis, respectively, but in the tetragonal structures O(2) = O(3).

The analysis of the O *K*-edge XANES spectra reveals numbers for hole concentrations, i.e., the relative peak intensities $I_{527.5}$ and $I_{528.2}$, which can be compared between the CuO_z chain and the CuO_2 plane in each sample as well as among the different samples, but the absolute values as such have no meaning. In order to make the relative numbers obtained from the XANES analysis more illustrative, all the $I_{527.5}$ and $I_{528.2}$ values were divided by a constant k. Furthermore, since the $I_{528.2}$ value denotes the sum of holes in two CuO_2 planes while the $I_{527.5}$ value is supposed to denote the number of holes in one CuO_z chain, the local CuO_2-plane and CuO_z-chain hole concentrations, $p_{\mathrm{XAS,plane}}$ and $p_{\mathrm{XAS,chain}}$ are given by

$$p_{\mathrm{XAS,plane}} = \frac{I_{528.2}}{2k} \quad [4]$$

and

$$p_{\mathrm{XAS,chain}} = \frac{I_{527.5}}{k}. \quad [5]$$

The constant k was artificially set to 0.7492 to yield a $p_{\mathrm{XAS,plane}}$ value equal to the $p_{\mathrm{BVS,plane}}$ value for the $x = 0$, $z = 0.96$ sample. Thus, if the present O *K*-edge XANES analysis and the BVS calculation method probed and correctly reflected the same quantity, the $p_{\mathrm{XAS,plane}}$s value should correspond to $p_{\mathrm{BVS,plane}}$ values for all the samples.

RESULTS AND DISCUSSION

The present $Cu(Ba_{0.8}Sr_{0.2})_2(Yb_{1-x}Ca_x)Cu_2O_{6+z}$ samples were of essentially single phase in the applied compositional ranges $0 \le x \le 0.35$ and $0 \le z \le 0.96$, as confirmed from the X-ray and neutron powder diffraction data (15, 16). In the XRD pattern of the Ca-free $Cu(Ba_{0.8}Sr_{0.2})_2YbCu_2O_6$ samples traces of the Yb_2BaCuO_5 impurity phase were detected, but according to the refinement of the NPD data, the contribution from the Yb_2BaCuO_5 structure was less than 1%. On the other hand, for the Ca-substituted samples reduced in Ar at 800°C slightly negative z values were obtained by coulometric titrations. These negative values could be explained by the presence of

TABLE 1

Oxygen Contents as Determined by Means of Wet-Chemical Analysis and T_c Values (in K) for the $Cu(Ba_{0.8}Sr_{0.2})_2(Yb_{1-x}Ca_x)Cu_2O_{6+z}$ Samples Together with Selected Bond Lengths (in Å) as Calculated from Neutron Powder Diffraction Data of Ref. (16)

x	0	0	0	0	0	0.10	0.20	0.25	0.35
z	0.06	0.38	0.55	0.76	0.96	~0	~0	~0	~0
T_c	<5	<5	37	55	82	<5	<5	27	43
Yb/Ca–O(2)	2.3662(11)	2.3666(14)	2.3728(21)	2.3828(18)	2.3864(14)	2.3741(11)	2.3749(8)	2.3857(8)	2.3888(8)
–O(3)	—	—	2.3726(14)	2.3631(14)	2.3577(11)	—	—	—	—
Ba/Sr–O(1)	3.0173(24)	3.0106(14)	2.9525(14)	2.9067(14)	2.8587(14)	3.0171(19)	3.0084(14)	3.0045(14)	3.0079(15)
–O(2)	2.8841(36)	2.8819(31)	2.9156(40)	2.9433(36)	2.9766(32)	2.8718(32)	2.8688(23)	2.8666(23)	2.8605(23)
–O(3)	—	—	2.8912(32)	2.9221(32)	2.9562(28)	—	—	—	—
–O(4)	2.7527(13)	2.7530(7)	2.7415(7)	2.7305(6)	2.7198(4)	2.7548(12)	2.7516(8)	2.7571(9)	2.7581(9)
Cu(1)–O(1)	1.9171(2)	1.9177(1)	1.9233(1)	1.9292(1)	1.9308(1)	1.9157(1)	1.9134(1)	1.9160(1)	1.9167(1)
–O(4)	1.8546(42)	1.8479(18)	1.8351(24)	1.8572(24)	1.8711(18)	1.8317(36)	1.8235(24)	1.8047(30)	1.8084(30)
Cu(2)–O(2)	1.9350(7)	1.9360(5)	1.9248(6)	1.9196(6)	1.9161(5)	1.9304(4)	1.9274(3)	1.9275(4)	1.9272(4)
–O(3)	—	—	1.9369(5)	1.9461(5)	1.9501(5)	—	—	—	—
–O(4)	2.3676(65)	2.3587(30)	2.3597(36)	2.3034(36)	2.2613(30)	2.4006(60)	2.4050(30)	2.4315(48)	2.4318(48)

trace amounts of an impurity phase of copper at the oxidation state +I (Cu_2O). However, no peaks due to Cu_2O were detected by the diffraction methods, and estimation for the oxygen excess from the NPD data ended up to z values in between 0 and 0.10. According to the TG data recorded for the Ar annealings, the oxygen content was very close to $z = 0$. For the following discussion, oxygen contents in these samples are given as $z \approx 0$. For other samples, z values were established from at least five parallel coulometric titrations. In Table 1, the stoichiometries and the T_c values for the investigated $Cu(Ba_{0.8}Sr_{0.2})_2(Yb_{1-x}Ca_x)Cu_2O_{6+z}$ samples are summarized together with selected bond lengths calculated for the samples from the NPD data of Ref. (16).

Based on the SQUID data obtained for the present samples and also for the more complete series of Ca-substituted and O-doped $Cu(Ba_{0.8}Sr_{0.2})_2(Yb_{1-x}Ca_x)Cu_2O_{6+z}$ samples of Ref. (15), it can be concluded that the Ca-free $Cu(Ba_{0.8}Sr_{0.2})_2YbCu_2O_{6+z}$ phase becomes superconductive when z exceeds ~ 0.45. With increasing z, T_c increases in a similar two-step manner as that established for the $CuBa_2YCu_2O_{6+z}$ system. On the other hand, upon increasing the Ca content x in the samples with $z \approx 0$ superconductivity appears at $x \approx 0.20$.

The Cu $L_{2,3}$-edge absorption spectra obtained for the samples are shown in Figs. 2(a) and 2(b). In the spectra shown in Fig. 2(b) for the oxygen-depleted $Cu(Ba_{0.8}Sr_{0.2})_2(Yb_{1-x}Ca_x)Cu_2O_{6.0}$ samples, a peak due to two-coordinated Cu^{I} around 934 eV is seen besides the two peaks due to Cu^{II} around 931 and 951 eV. The intensity of this 934 eV peak remains rather unchanged with increasing Ca-substitution level x, demonstrating that Ca substitution does not oxidize the charge-reservoir Cu(1) atoms. On the other hand, with the amount of excess oxygen increasing in the $Cu(1)O_z$ chain, the peak at 934 eV disappears around $z \approx 0.55$ (Fig. 2(a)), i.e., the portion of Cu^{I} becomes insignificant. Upon increasing the oxygen content, a shoulder arising from Cu^{III} appears on the high-energy side of the main peak at ~ 931 eV. With increasing z, the 931 eV peak becomes increasingly asymmetric, indicating a considerable increase in the total portion of Cu^{III}, at the CuO_2-plane Cu(2) site and/or at the CuO_z-chain Cu(1) site. On the other hand, with Ca substitution no prominent increase in the amount of Cu^{III} is seen. For the Ca-free samples, the 931 eV peak and its shoulder were analyzed by fitting with two Gaussian functions, as demonstrated in Fig. 2(c) for the $x = 0$, $z = 0.96$ sample. The results are given in Table 2 and also plotted in Fig. 3 against z. From Fig. 3, with increasing z the relative intensity of the shoulder increases in a continuous but not totally linear manner. It seems that initially (with $z < 0.4$) the excess oxygen atoms oxidize more strongly the charge-reservoir $Cu(1)^{I}$ atoms (to Cu^{II} or Cu^{III}) than the

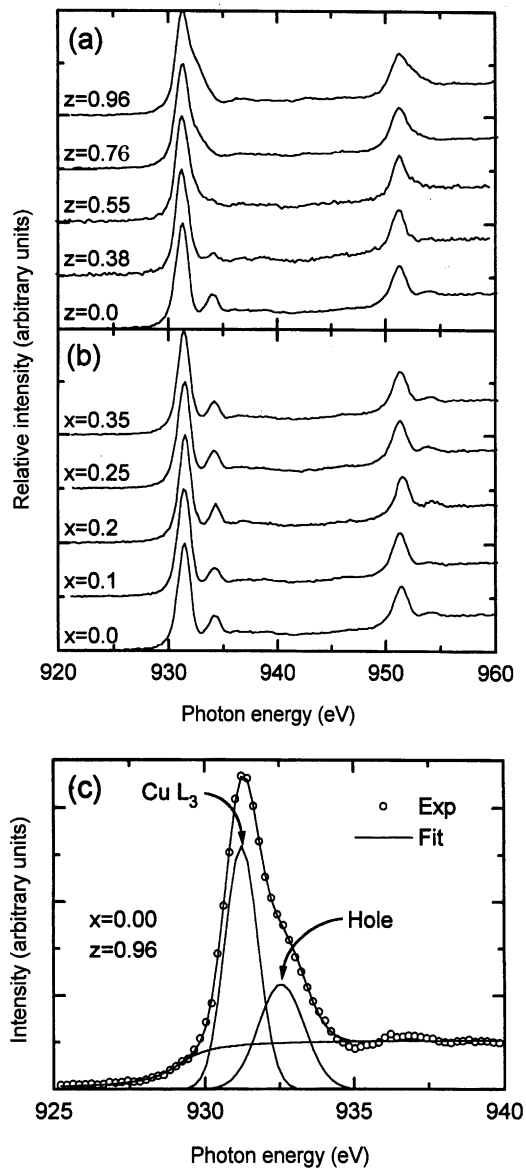

FIG. 2. The Cu $L_{2,3}$-edge XANES spectra for the sample series (a) $Cu(Ba_{0.8}Sr_{0.2})_2YbCu_2O_{6+z}$ and (b) $Cu(Ba_{0.8}Sr_{0.2})_2(Yb_{1-x}Ca_x)Cu_2O_{6.0}$ in the energy range 920–960 eV, and (c) the fitting of the L_3 spectrum with Gaussian components for the $x = 0$, $z = 0.96$ sample.

CuO_2-plane $Cu(2)^{II}$ atoms (to Cu^{III}), as the rate of detected Cu^{III}, i.e., increasing $I_{932.6}$, against increasing z is lower for the smaller z values. This is consistent with the fact that with increasing z the peak at 934 eV due to two-coordinated Cu^{I} was found to disappear already around $z \approx 0.55$.

The O K-edge spectra obtained for the $Cu(Ba_{0.8}Sr_{0.2})_2(Yb_{1-x}Ca_x)Cu_2O_{6+z}$ samples are shown in Figs. 4(a) and 4(b). As described in detail in Experimental, the pre-edge features were assigned and analyzed in the way proposed/applied in Refs. (4–10) (see Fig. 4(c) for the case of $x = 0$,

TABLE 2

The Fitted Relative Values for the Peak Areas of the O *K*-Edge XANES Peaks at ~527.5 eV ($I_{527.5}$), ~528.2 eV ($I_{528.2}$) and ~529.2 eV ($I_{529.2}$), and the Cu L_3-Edge XANES Peak at ~932.6 eV ($I_{932.6}$) (Only for the $x = 0$ Samples) for the $Cu(Ba_{0.8}Sr_{0.2})_2(Yb_{1-x}Ca_x)Cu_2O_{6+z}$ Samples

Sample		O *K*-edge			Cu L_3-edge
x	z	$I_{527.5}$ (chain)	$I_{528.2}$ (plane)	$I_{529.2}$ (UHB)	($I_{932.6}$)
0	0.06	0.0	0.0	0.327	0
0	0.38	0.011	0.015	0.302	0.103
0	0.55	0.102	0.140	0.306	0.304
0	0.76	0.180	0.261	0.218	0.424
0	0.96	0.321	0.457	0.147	0.651
0.10	~0	0.0	0.0	0.260	—
0.20	~0	0.003	0.024	0.306	—
0.25	~0	0.005	0.037	0.268	—
0.35	~0	0.009	0.051	0.216	—

$z = 0.96$). The obtained relative intensities for the three pre-edge peaks are given in Table 2. The integrated intensity of the pre-edge peak at ~528.2 eV, $I_{528.2}$, which directly reflects the concentration of holes in the CuO_2 plane, increases continuously with increasing z/x within the whole doping/substitution range indicating that the CuO_2-plane hole concentration also increases continuously as O doping or Ca substitution proceeds. Simultaneously, the peak at ~529.2 eV due to UHB becomes smaller. Similar behavior has been observed for other p-type superconductive copper oxides. For the exact position of the ~528.2 eV pre-edge peak, a tendency of decreasing absorption energy with increasing doping/substitution level is observed for both O doping and Ca substitution, suggesting that the Fermi level shifts to lower energies with increasing hole concentration in the CuO_2 plane.

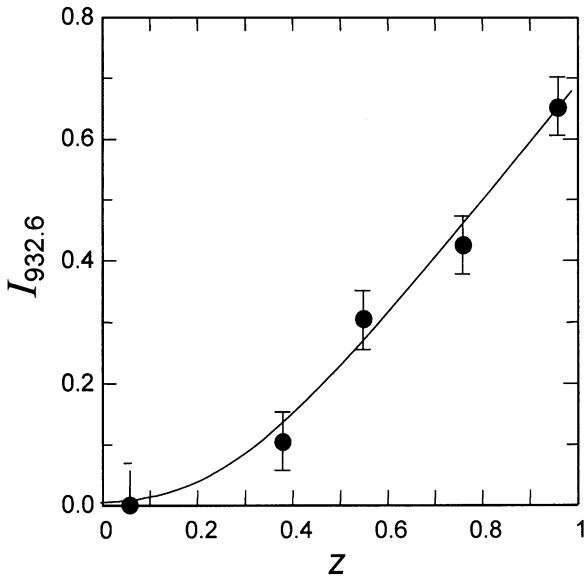

FIG. 3. The fitted relative values for peak areas of the Cu L_3-edge XANES peak at ~932.6 eV ($I_{932.6}$) for the Ca-free $Cu(Ba_{0.8}Sr_{0.2})_2YbCu_2O_{6+z}$ samples with increasing z. The error bars shown are rough estimations based on an assumption that the experimental precision of the data points including the measurement and fitting errors is 5–10%.

In Table 3, the values are summarized for the local CuO_z-chain and CuO_2-plane hole concentrations calculated for the $Cu(Ba_{0.8}Sr_{0.2})_2(Yb_{1-x}Ca_x)Cu_2O_{6+z}$ samples from the O *K*-edge XANES data, i.e., $p_{XAS,chain}$ and $p_{XAS,plane}$, and those for the CuO_2-plane hole concentrations from the NPD data through BVS calculation, i.e., $p_{BVS,plane}$. Even though the absolute values of $p_{XAS,plane}$ and $p_{BVS,plane}$ obtained for one sample slightly differ, both the values show similar trends among the samples. From Table 3, the major difference between the two hole-doping ways, i.e., O doping and Ca substitution, is that with Ca substitution the holes are directed mainly into the CuO_2 plane while with O doping the hole concentration increases rather strongly in the CuO_z chain. Moreover, the value of T_c seems to depend on the way that has been used to dope the holes. In Figs. 5(a) and 5(b), respectively, the value of T_c is plotted against $p_{XAS,plane}$ and $p_{BVS,plane}$ for the two sample series, i.e., O-doped and Ca-substituted $Cu(Ba_{0.8}Sr_{0.2})_2(Yb_{1-x}Ca_x)Cu_2O_{6+z}$ samples. Both plots clearly reveal the same trend, that is, at a certain hole-concentration value the T_c value is higher for the Ca-substituted sample than for the O-doped sample. This inevitably means that besides the local hole concentration of the CuO_2 plane, other factors also contribute in determining the superconductivity properties of multi-layered copper oxides. In the present $Cu(Ba_{0.8}Sr_{0.2})_2(Yb_{1-x}Ca_x)Cu_2O_{6+z}$ system, Ca substitution and O doping were clearly demonstrated to result in different homogeneities of the hole distribution. They are also likely to result in

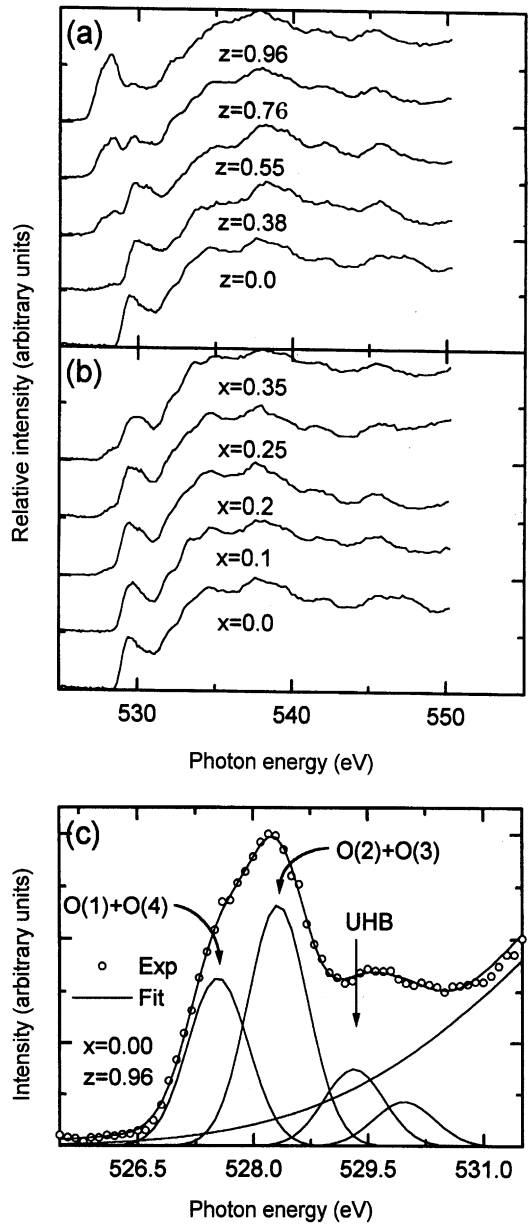

FIG. 4. The O *K*-edge XANES spectra for the sample series (a) $Cu(Ba_{0.8}Sr_{0.2})_2YbCu_2O_{6+z}$ and (b) $Cu(Ba_{0.8}Sr_{0.2})_2(Yb_{1-x}Ca_x)Cu_2O_{6.0}$ in the energy range 525–550 eV, and (c) the fitting of the pre-edge peaks below 531 eV with Gaussian components for the $x = 0$, $z = 0.96$ sample.

different distributions of holes between the in-plane copper and oxygen atoms. The fact that the optimized value of T_c varies considerably among different copper oxide superconductors has been attributed to such a phenomenon (1, 3, 21, 22). By the choice of the way of doping the CuO_2 plane(s) with holes it should be possible to control the different factors determining the superconductivity characteristics (3).

TABLE 3

Different Hole Concentration Values in the $Cu(Ba_{0.8}Sr_{0.2})_2(Yb_{1-x}Ca_x)Cu_2O_{6+z}$ Samples: $p_{XAS,chain}$, $p_{XAS,plane}$, and $p_{BVS,plane}$ as Calculated from the O *K*-Edge XANES Data and from the NPD Data by the BVS Method, Respectively

Sample				
x	z	$p_{XAS,chain}$	$p_{XAS,plane}$	$p_{BVS,plane}$
0	0.06	0	0	0.084
0	0.38	0.015	0.010	0.085
0	0.55	0.136	0.093	0.148
0	0.76	0.240	0.174	0.229
0	0.96	0.429	0.305	0.305
0.10	~0	0	0	0.074
0.20	~0	0.004	0.016	0.069
0.25	~0	0.007	0.025	0.092
0.35	~0	0.012	0.034	0.089

CONCLUSIONS

For superconductive multi-layered copper oxides $M_mA_2Q_{n-1}Cu_nO_{m+2+2n-\delta}$, distribution of holes over different layers/blocks is an essential parameter since together with the overall hole-doping level it controls the superconductivity characteristics. However, there has been no single well-established analysis technique that could probe explicitly the distinct hole concentrations of different structural blocks. In this work, we presented the results of applying O *K*-edge and Cu $L_{2,3}$-edge XANES spectroscopy to two series of $Cu(Ba_{0.8}Sr_{0.2})_2(Yb_{1-x}Ca_x)Cu_2O_{6+z}$ samples in which the holes were generated in different ways, i.e., by Ca substitution and O doping. Application of XANES spectroscopy allowed us to determine the distribution of holes between the CuO_2–$(Yb_{1-x}Ca_x)$–CuO_2 block containing two identical superconductive CuO_2 planes and the charge-reservoir block consisting of a single CuO_z chain. For each sample studied, the oxygen content was accurately analyzed by means of wet-chemical analysis and further confirmed from the oxygen occupancy factors derived from neutron diffraction data. Comparison of the resultant values of the local hole concentration with those estimated for the same samples through BVS calculation from the neutron diffraction data revealed that the results obtained by these two independent methods were highly consistent. It was, furthermore, concluded that the holes generated via Ca substitution are directed efficiently into the CuO_2 plane while with O doping the hole concentration increases rather strongly in the CuO_z chain. Moreover, the value of T_c was shown to depend not only on the CuO_2-plane hole concentration but also on other factors such that, at a fixed CuO_2-plane hole concentration, substitution of Yb^{III} by Ca^{II} facilitated a higher T_c value than doping with oxygen.

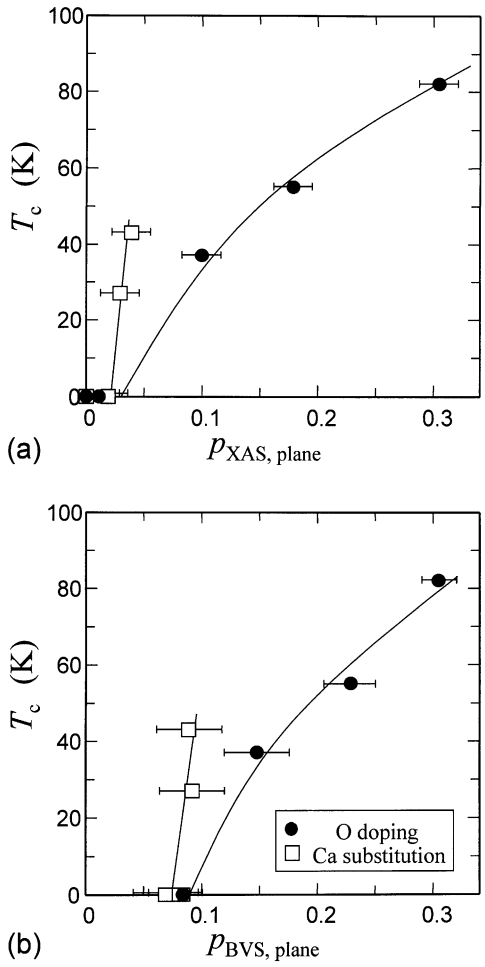

FIG. 5. The dependence of T_c on the CuO_2-plane hole concentration as estimated from (a) the O *K*-edge XANES data, and (b) the NPD data through BVS calculation for the two different sample series, i.e., O-doped and Ca-substituted $Cu(Ba_{0.8}Sr_{0.2})_2(Yb_{1-x}Ca_x)Cu_2O_{6+z}$ samples. Note that the $p_{XAS,plane}$ values were standardized such that the $p_{XAS,plane}$ value would be equal to the $p_{BVS,plane}$ value for the $x = 0$, $z = 0.96$ sample. The error bars for $p_{BVS,plane}$'s have been estimated from the standard deviations of the corresponding bond lengths given in Table 1, while for $p_{XAS,plane}$'s 5–10% error bars are assumed.

ACKNOWLEDGMENTS

Helpful discussions with Prof. R. Tellgren and Dr. H. Rundlöf of Uppsala University are gratefully acknowledged. This work was supported by Grant-in-Aid for Scientific Research (Contract No. 11305002) from the Ministry of Education, Science and Culture of Japan, International Collaborative Research Project Grant-2000 of the Materials and Structures Laboratory, Tokyo Institute of Technology, and also by Academy of Finland (Decision No. 46039).

REFERENCES

1. M. Karppinen and H. Yamauchi, *Mater. Sci. Eng. R* **26,** 51–96 (1999).
2. M. Karppinen, A. Fukuoka, L. Niinistö, and H. Yamauchi, *Supercond. Sci. Technol.* **9,** 121–135 (1996).
3. M. Karppinen and H. Yamauchi, *Int. J. Inorg. Mater.* **2,** 589–599 (2000).
4. N. Nücker, E. Pellegrin, P. Schweiss, J. Fink, S. L. Molodtsov, C. T. Simmons, G. Kaindl, W. Frentrup, A. Erb, and G. Müller-Vogt, *Phys. Rev. B* **51,** 8529–8542 (1995).
5. J. M. Chen, R. G. Liu, S. C. Chung, R. S. Liu, M. J. Kramer, K. W. Dennis, and R. W. McCallum, *Phys. Rev. B* **55,** 3186-3191 (1997).
6. M. Merz, N. Nücker, E. Pellegrin, P. Schweiss, S. Schuppler, M. Kielwein, M. Knupfer, M. S. Golden, J. Fink, C. T. Chen, V. Chakarian, Y. U. Idzerda, and A. Erb, *Phys. Rev. B* **55,** 9160–9172 (1997).
7. J. M. Chen, R. S. Liu, J. G. Lin, C. Y. Huang, and J. C. Ho, *Phys. Rev. B* **55,** 14 586–14 591 (1997).
8. R. S. Liu, C. Y. Chang, and J. M. Chen, *Inorg. Chem.* **37,** 5527–5531 (1998).
9. R. S. Liu, C. Y. Chang, J. M. Chen, and R. G. Liu, *J. Supercond.* **11,** 563–567 (1998).
10. J. M. Chen, R. S. Liu, P. Nachimuthu, M. J. Kramer, K. W. Dennis, and R. W. McCallum, *Phys. Rev. B* **59,** 3855–3861 (1999).
11. I. J. Hsu, R. S. Liu, J. M. Chen, R. G. Liu, L. Y. Jang, J. F. Lee, and K. D. M. Harris, *Chem. Mater.* **12,** 1115–1121 (2000).
12. M. Karppinen, M. Kotiranta, H. Yamauchi, P. Nachimuthu, R. S. Liu, and J. M. Chen, *Phys. Rev. B* **63,** 184 507–184 512 (2001).
13. M. Merz, N. Nücker, P. Schweiss, S. Schuppler, C. T. Chen, V. Chakarian, J. Freeland, Y. U. Idzerda, M. Kläser, G. Müller-Vogt, and Th. Wolf, *Phys. Rev. Lett.* **80,** 5192–5195 (1998).
14. T. Wada, Y. Yaegashi, A. Ichinose, H. Yamauchi, and S. Tanaka, *Phys. Rev. B* **44,** 2341–2347 (1991).
15. K. Fujinami, M. Karppinen, and H. Yamauchi, *Physica C* **300,** 17–25 (1998).
16. M. Karppinen, H. Yamauchi, K. Fujinami, T. Nakane, K. Peitola, H. Rundlöf, and R. Tellgren, *Phys. Rev. B* **60,** 4378–4385 (1999).
17. Z. Hu, G. Kaindl, S. A. Warda, D. Reinen, F. M. F de Groot, and B. G. Müller, *Chem. Phys.* **232,** 63–74 (1998).
18. A. Bianconi, M. DeSantis, A. Di Ciccio, A. M. Flank, A. Fronk, A. Fontaine, P. Legarde, H. K. Yoshida, A. Kotani, and A. Marcelli, *Phys. Rev. B* **38,** 7196–7199 (1988).
19. M. Grioni, J. B. Goedkoop, R. Schoorl, F. M. F. de Groot, J. C. Fuggle, F. Schäfers, E. E. Koch, G. Rossi, J.-M. Esteva, and R. C. Karnatak, *Phys. Rev. B* **39,** 1541–1545 (1989).
20. I. D. Brown and D. Altermatt, *Acta Crystallogr. B* **41,** 244–247 (1985).
21. J. L. Tallon, *Physica C* **168,** 85–90 (1990).
22. G. Zheng, Y. Kitaoka, K. Asayama, K. Hamada, H. Yamauchi, and S. Tanaka, *Physica C* **260,** 197–210 (1996).